INVESTIGATION OF AEROELASTIC STABILITY PHENOMENA OF A HELICOPTER BY IN-FLIGHT SHAKE TEST

Wen-Liu Miao, W. Thomas Edwards, and David E. Brandt
Boeing Vertol Company

ABSTRACT

The aeroelastically stable Boeing YUH-61A helicopter was developed through a systematic program of configuration analysis and model testing which has resulted in a successful flight test program. The analytical capability of the helicopter stability program, C-56, is discussed. The parameters which are found to be critical to the air resonance characteristics of the soft in-plane hingeless rotor systems are detailed.

A summary of two model test programs, a 1/13.8 Froude-scaled BO-105 model and a 1.67 meter (5.5 foot) diameter Froude-scaled YUH-61A model, are presented. Emphasis is placed on the selection of the final parameters which were incorporated in the full scale YUH-61A helicopter, and model test data for this configuration are shown.

The actual test results of the YUH-61A air resonance in-flight shake test stability are then presented. This includes a concise description of the test setup, which employs the Grumman Automated Telemetry System (ATS), the test technique for recording in-flight stability, and the test procedure used to demonstrate favorable stability characteristics with no in-plane damping augmentation (lag damper removed). The data illustrating the stability trend of air resonance with forward speed and the stability trend of ground resonance for percent airborne are presented.

INTRODUCTION

The successful development of a helicopter with a soft in-plane hingeless rotor system requires that certain potential aeroelastic stability problems be examined, in particular the air and ground resonance phenomena. Both air and ground resonance are coupled rotor/airframe instabilities which may occur when the natural aircraft body pitch or roll frequency, involving hub motion, is equal to or close to the difference between rotor speed and the in-plane natural frequency. However, with the proper choice of certain critical rotor parameters, such as, blade precone, pitch-flap coupling, pitch-lag coupling, control system stiffness, and blade in-plane natural frequency, the stability of the coupled rotor/airframe can be controlled. This has already been demonstrated with the Boeing Messerschmitt-Boelkow-Blohm BO-105 helicopter.

19

For the development of the Boeing Vertol YUH-61A helicopter, a systematic approach was made to the aeroelastic design of the aircraft which results in the optimization of the critical parameters. The approach entails:

Computer analysis of stability characteristics

Preliminary model testing, to correlate analysis and determine the most influential stability parameters

Detailed model testing of the proposed configuration

Flight envelope expansion of the full scale helicopter by determining degree of stability through in-flight shake test

The YUH-61A stability testing was performed at the Grumman Aerospace Corporation facility at Calverton, Long Island. To expedite this work and to promote minimum risk, the Grumman Automated Telemetry System (ATS) was used to provide on-line real-time analysis of the data.

Many of the model test data were presented in previous papers. For the sake of completeness, portions of those works are summarized herein.

The authors express their appreciation to W. F. White and C. E. Hammond of the U. S. Army Air Mobility Research and Development Laboratory at Langley for their help with processing and verifying the YUH-61A flight test data with the moving block/Randomdec computer program.

ANALYSIS

A method for determining the ground resonance characteristics of a helicopter with an articulated rotor (Reference 1) has existed for over thirty years. Analyses of this type considered only the resonance of the forces generated by blade cyclic in-plane motions with a single effective hub mass restrained to move in two translational directions without aerodynamic effects. This translating, effective hub mass attempted to represent a modal combination of hub and airframe translations and pitching and rolling motions. These pitching and rolling motions are of little consequence in the analysis of a rotor with small flap hinge offsets. However, if there is a sizeable effective flap hinge offset, as in the case of a hingeless rotor system, these motions produce large aerodynamic flapping moments which can damp the ground resonance or related air resonance modes (Reference 2). Therefore, the pitching and rolling motion as well as the aerodynamic consideration become indispensable for the hingeless rotor system. The C-56 program was developed to provide this more exact representation.

Analytical Capability (C-56 Program)

The C-56 analysis retains the degrees of freedom of the helicopter rotor and airframe which influence the air and ground resonance characteristics. This relatively simple but adequate analytical representation includes these pertinent freedoms:

Three rigid-body fuselage translations

Two rigid-body fuselage rotations (pitch and roll)

Four mast or pylon motions (lateral and longitudinal translations, pitch, and roll) defined at the softest pylon-to-fuselage junction

Two tail boom flexibilities

Nine rotor freedoms (one collective and two cyclic modes for blade pitching, flapping, and in-plane motions) (excludes reactionless modes)

A drawing of the 20 degrees of freedom is shown in Figure 1.

The equations of motion for this entire multidimensional system are derived from Lagrange's equations. A brief discussion of this derivation was presented in Reference 3.

This representation permits the investigation of a wide range of parameters affecting rotor/airframe stability. In addition to making it possible to study the effects of basic characteristics, such as rotor speed, rotor thrust, aircraft gross weight, forward speed (in an extended version of the program), and Lock number, the representation makes it possible to examine the following parameters: precone, control system stiffness, lag frequency, and pitch-lag and pitch-flap coupling terms. Although other parameters may also be investigated, these in particular have a strong influence on stability.

Parameter Sensitivity

The mechanism of the air and ground resonance of the hingeless rotor helicopter and its attendant source of damping were discussed elsewhere, e.g., Reference 2. It suffices to say that since the prime source of damping in the air and ground resonance mode is the blade flap response, any parameter which affects the coupled blade feather, flap, and lag motions has the potential for stabilizing or destabilizing the mode. A sensitivity study revealed that the favorable couplings were nose-up pitch and upward flap, both of which caused blade lag, and upward flap, which caused nose-down pitch. Any hub geometry and blade design which result in these three types of coupling in a soft in-plane rotor system will beneficially affect the air resonance stability. Let us now examine some of the most common design parameters.

Precone. Precone here means the precone of the blade feathering axis. Figure 2 shows the precone effect on the YUH-61A air resonance mode stability. As the blade feathering axis precones up towards the equilibrium position, the modal damping decreases.

As discussed in Reference 2, with the blade feathering bearing inboard of the blade flexure, precone of the blade feathering axis directly controls the magnitude of the flap-pitch coupling caused by the Coriolis force. The perturbation Coriolis force due to flapping up velocity acts toward the leading edge of the blade. With the blade equilibrium position above the feathering axis producing a moment arm, there results a nose-down perturbation pitching moment, which is favorable. Figure 3 shows schematically the reduction of the moment arm with increasing precone; hence the reduction of the favorable flap-pitch coupling.

Control system flexibility. Figure 4 shows the effect of the control system flexibility on the air resonance mode stability of the YUH-61A. Comparing the stiff control system to the nominal control system, we see that the former degrades the stability for collective pitch from 25 to 240 percent of hover 1g collective (θ_{NOR}) and enhances the stability from then on up.

Since the stability is influenced by the blade flap-pitch and pitch-lag coupling, its dependence on the control system flexibility is expected. As discussed in Reference 2, there exists favorable flap-pitch coupling for the low collective pitch region, in this case from 25 to 200 percent θ_{NOR}, and unfavorable coupling at high collective pitch, in this case from 200 percent on up. The stiff control system minimizes the coupling effect and therefore produces the trend shown in Figure 4. The choice of the control system stiffness therefore depends on the practical operational collective pitch range for which the rotor is designed.

Lag frequency. There are several factors which have a primary influence on the air and ground resonance characteristics of the helicopter. One of these is the placement of the lag frequency with respect to the coupled airframe pitch-dominant and roll-dominant modes. This has been discussed for an aircraft with a gross weight of about 2045 kg (4500 pounds) in Reference 4.

As stated in that reference, there are two potential resonance points which are, in general, detrimental to aircraft air resonance characteristics. These points, shown in Figure 5, should be avoided for all flight conditions of the particular aircraft. However, there are two possible stable regions of rotor operation which are available for a given helicopter design. Both of these regions now have been shown to provide satisfactory stability margins, with the Boeing YUH-61A designed for region 1 and the MBB BO-105 designed for region 2.

The choice of the optimum operating region for these helicopters indirectly results from the aircraft mission. The mission profile sizes the rotor system, aircraft gross weight, and pitch and roll inertias. The roll predominant and pitch-predominant modes are strongly coupled with the rotor cyclic flapping, which provides the stiffness for those directions in flight. Therefore, with the aircraft pitch- and roll-predominant modes fixed by the above considerations, the in-plane blade stiffness, and therefore lag frequency and $\Omega - \omega_\zeta$, is then chosen to meet rotor load requirements and to place the rotor speed in the center of one of the operating regions.

YUH-61A Analytical Results

For the final YUH-61A configuration, the various beneficial parameters are combined to produce a stable configuration. A summary of the key rotor and fuselage parameters is shown in Table 1.

Table 1 Summary of YUH-61A Parameters

Parameter	Value
In-plane Frequency (ω_ζ)	0.70 per N_R (Normal Rotor Speed)
Pitch-Flap Coupling (δ_3)	-22.5° (Flap Up-Pitch Nose Down)
Precone	0°
Droop	3.25° Up
Blade Torsion Frequency (ω_θ)	3.76 per N_R
Rigid Airframe Roll Frequency	0.366 per N_R
Rigid Airframe Pitch Frequency	0.095 per N_R
In-plane Damping Augmentation	0% (In-plane Structural Damping ≈ 1.0%)
Landing Gear Damping Augmentation	0%

These parameters were modeled for the C-56 program, and air resonance and ground resonance characteristics were determined. A plot of the predicted air resonance stability as a function of thrust and rotor speed is shown in Figure 6. The low RPM boundary in this plot corresponds to the resonance of $\Omega - \omega_\zeta$ with the pitch-dominant mode, and the high RPM boundary corresponds to the resonance of the $\Omega - \omega_\zeta$ mode and the roll-predominant mode. The reduction in stability at high thrust (or collective pitch) levels is due to detrimental flap-pitch coupling in this region, as explained in Reference 2.

The results of the ground resonance analysis as a function of percent airborne is shown in Figure 7. This plot displays the Ω-ω_ζ mode modal damping for three different rotor speeds ranging from the aircraft's minimum value (N_{min}) to the maximum design limit speed (N_{DL}). This completely covers the range explored later on the first test vehicle.

MODEL TESTS

The model tests performed in conjunction with the development of an aeroelastically stable YUH-61A configuration were conducted in two parts.

1/13.8 Froude-scaled BO-105 model

1.67 meter (5.5 foot) diameter Froude-scaled YUH-61A model

Froude-Scaled BO-105 Model

This 1/13.8 Froude-scaled BO-105 model (Reference 2) was developed to provide a direct means of validating the analytical methods detailed above and to demonstrate the power of the several rotor parameters to influence aircraft air resonance characteristics. The model has the same blade first flap, lag, and torsion frequencies as full scale, with provisions to vary hub precone, blade sweep, and blade lag damping to observe their effects on rotor stability. The model parameters are summarized in the following table.

Table 2 1/13.8 Scale BO-105 Model Parameters

Parameter	Value
Rotor Diameter	71 cm (28 in.)
Chord	1.94 cm (0.762 in.)
Gross Weight	0.85 kg (1.87 lb)
Precone	Variable
ω_β/Ω (Flap)	1.12
ω_ζ/Ω (Lag)	0.62
ω_θ/Ω (Pitch)	3.6
Roll Inertia	0.456×10^{-3} m-kg-sec^2 (0.0395 in-lb-sec^2)
Pitch Inertia	1.224×10^{-3} m-kg-sec^2 (0.106 in-lb-sec^2)

The air resonance characteristics for this model are determined primarily by the frequency placement as a function of rotor speed of the significant modes: (a) $\Omega-\omega_\zeta$, the air resonance mode; (b) aircraft pitch, rigid body pitch restrained by rotor flap; and (c) aircraft roll, rigid body roll restrained by rotor flap, as detailed in the previous section of the lag frequency sensitivity. The plot of these modal frequencies and the related modal damping versus rotor speed is shown in Figure 8.

At a given rotor speed the variation of rotor thrust, or collective pitch, produces changes in $\Omega-\omega_\zeta$ mode modal damping. A typical plot of this effect is shown in Figure 9. The modal damping plot of $\Omega-\omega_\zeta$ shows two possible regions of model instability. The first is at low collective, from 30 percent to 50 percent of hover 1g collective, and reflects the mild reduction in the stability of the isolated rotor lag mode. The second, high collective region displays a steep modal damping gradient which is created by detrimental flap-pitch coupling at the high thrust (Reference 2).

The importance of both rotor speed and maneuver thrust on air resonance characteristics was realized, so the model was tested through a wide range of rotor speeds and thrust conditions. The stability observed at these conditions was correlated with analytical stability boundaries. A typical map of this type is shown in Figure 10. In addition to lending confidence in the analytical methods, this test and analytic work confirmed the power of several rotor parameters to enhance and control air resonance stability characteristics (Reference 2). These parameters are as follows:

Precone of the blade feathering axis

Control system flexibility

Lag damping

1.67 Meter (5.5. Foot) Diameter Froude-Scaled YUH-61A Model

The next step in the development of the aeroelastically stable YUH-61A configuration is the testing of a 1.67 meter (5.5 foot) diameter model (Reference 5). This soft in-plane hingeless rotor system was tested on a gimbal which allowed the helicopter rigid-body pitch and roll motions. The rotating frequencies of this model are scaled to full scale and therefore are different from those of the BO-105 Froude-scaled model. A summary of the model parameters appear in Table 3.

Table 3 Summary of 1.67 Meter Diameter Model Parameters

Parameter	Value
Rotor Diameter	1.67 m (5.5 ft)
Chord	6.6 cm (2.6 in.)
Gross Weight	17.64 kg (38.8 lb)
Precone	Variable
ω_β/Ω (Flap)	1.09
ω_ζ/Ω (Lag)	0.67
ω_θ/Ω (Pitch)	4.30
Roll Inertia	0.01479 m-kg-sec^2 (1.281 in.-lb-sec^2)
Pitch Inertia	0.08844 m-kg-sec^2 (7.66 in.-lb-sec^2)

Figure 11 shows the nondimensional natural frequencies as a function of rotor speed for this model. Comparison of this figure and Figure 8 reveals that the basic difference between the two models is the placement of the roll-predominant mode. In the 1.67 meter (5.5 foot) diameter configuration, the coalescence of the roll-predominant mode and the Ω-ω_ζ mode occurs slightly beyond 120 percent normal rotor speed (N_R).

Tests of the model in hover determined that two unstable regions similar to those predicted by analysis were present (Figure 6). In a typical map of test points in hover, Figure 12 demonstrates the boundaries: one is at about 70 percent of normal rotor speed and 120 percent of normal collective pitch, corresponding to the resonance with the body-pitch-predominant mode, and one is at 135 percent RPM and 100 percent collective, corresponding to the resonance with the body-roll-predominant mode.

The stability of the air resonance mode was also explored with respect to forward speed using the 1.67 meter diameter model. A plot of the test data at level flight trim collective pitch is presented in Figure 13. Because of the instrumentation arrangement during this phase of testing, the damping values were recorded from the rate of decay exhibited in the chord bending gage. The time to half amplitude observed in this way is equal to that of the Ω-ω_ζ air resonance mode. However, the frequency in the rotating system is ω_ζ, and therefore the data must be multiplied by the ratio of $\omega_\zeta/(\Omega-\omega_\zeta)$ to represent the air resonance mode damping. This is demonstrated and is shown in Figure 17, a typical time history of the YUH-61A in-flight shake test results.

During this test program, the test technique employed to obtain these data was refined. It was determined at the time that by exciting the model with lateral stick deflections in a sinusoidal fashion at a frequency of Ω-ω_ζ, the mode of interest could be observed. A typical time history which demonstrates this method of excitation and the measurement of damping is shown in Figure 14. As shown in this figure, the excitation produces a characteristic $\Omega-\omega_\zeta$ modal response characterized by the lead-lag motions of the blades at ω_ζ (observed in the rotating system) and by body roll and pitch motion at $\Omega-\omega_\zeta$ (observed in the fixed system).

In addition, the optimum values for the rotor and airframe parameters were determined for incorporation in the full scale design. These were presented in Table 1 in the previous section.

YUH-61A FLIGHT TEST

The YUH-61A stability testing was performed at the Grumman Aerospace Corporation facility at Calverton, Long Island (Figure 15). It was conducted during the envelope expansion phase of the flight test program. Because of the test technique adopted, which enables the determination of modal damping or degree of stability at every test point, in conjunction with the test setup and the test procedure employed, this in-flight stability shake test is truly a minimum risk program.

Test Setup

To expedite this work and to promote minimum risk, the Grumman Automated Telemetry System (ATS) was used to provide on-line real-time analysis of the data.

This data system has a wide range of operational capabilities (Reference 6), one of which is rotor system stability investigation. A schematic representation of the flow of information from the test aircraft to the data analyst is shown in Figure 16.

A frequency-modulated (FM) hybrid telemetry system is installed in the test aircraft. The transmitted signal includes flight-crew voice communications, a pulse-code-modulated (PCM) data set, an FM data set, and a time-code-generation signal. The primary data parameters which are observed and measured for the stability testing are as follows: chordwise bending moment from all four blades; flapwise bending moment; blade torsional moment; main transmission lateral and longitudinal accelerations; lateral and longitudinal stick positions; lateral and longitudinal stability and control augmentation system (SCAS) output; pitch, roll, and yaw of helicopter; pitch, roll, and yaw rates.

During a test flight, this raw signal is continuously recorded on magnetic tape in the ground station. In addition, a pilot-controlled on-board magnetic tape records these data plus additional data sets.

The ATS computers control the flow of information from the telemetry data stream to the analytical station. For a given test event, the analyst determined the level of inherent stability from two ATS output systems. The primary system is a real-time digital computer analysis of the rate of decay of the critical parameters from an initially excited state. The results of the analysis are displayed at the data analyst's station (DAS) on a cathode-ray tube (CRT) display.

As a backup to this system and to provide supplemental analytic capability, strip charts are utilized. The strip charts were found particularly useful in evaluating the quality of data being analyzed in terms of the contamination of the pure modal decay by random gusts. A more detailed explanation of DAS operation is presented in Reference 6.

Test Technique

The test technique employed to determine inherent stability levels for the YUH-61A was developed through model testing. This technique involves basically the following sequence:

Establish test condition

Turn on recording system

Turn on excitation

Turn off excitation

Record convergence of aircraft motions

Analyze data to obtain modal damping

Proceed to new test condition

The excitation for each test condition is supplied by a shaker system directly connected to the aircraft control system. The shaker is constructed with manual pilot-controlled selection of the shaker frequency, the axis of excitation, the shaker authority or gain, and the on-off controls. The output of the shaker is fed directly to the aircraft swashplate; therefore the required excitation frequency to the swashplate is $\Omega-\omega_\zeta$, which in turn excites the blade at ω_ζ, producing response in the air resonance mode.

During these tests the axis of excitation was limited to purely lateral or purely longitudinal. The tests of the 1.67 meter diameter model indicated that lateral excitation is the most responsive direction for the air resonance mode; for example, see Figure 14. Therefore, after this was confirmed on the flight test vehicle during the initial test conditions, the lateral excitation was used exclusively. A stick whirl excitation induced manually by pilot was used at the suggestion of C. E. Hammond of Langley. This resulted in quite satisfactory test results.

Figure 17 shows the time history of a typical test event. The time histories from the top down are blade chordwise bending, filtered chordwise bending, filtered main transmission lateral acceleration, SCAS (or shaker) input, and main rotor one per rev. The chord bending reflects the blade lead-lag motion in the rotating system, while the transmission lateral reflects the body lateral roll motion in the fixed system. Because of the closeness in frequency of the main rotor speed and the first in-plane natural frequency, even with a low pass filter, the one per rev forced response is still evident in the filtered chord bending trace. However, if this residual forced response is subtracted from the total chord bending response, the time for the chord motion to decay to half amplitude is the same as the time for the transmission lateral motion. This is expected, since the components of the physical system should decay at the same rate when a pure mode is excited. Modal damping can be obtained from either the chord bending or the transmission lateral, with the restraint that the reference frequency is $\Omega-\omega_\zeta$, not ω_ζ. Note also that the filtered traces have a time lag as compared to the excitation stop point, partly because of the low pass filters used.

Test Procedure

A maximum effort has been made throughout the entire YUH-61A development program to maintain minimum risk while providing and demonstrating adequate air resonance mode stability margins. During the actual flight test program, this was accomplished by the temporary addition of high in-plane damping (6 percent critical damping) to the rotor system by using lag dampers and by the temporary use of high damping landing gear shock struts.

The YUH-61A design configuration, because of the choice of the key rotor parameters, requires no lag dampers or landing gear damping. This was demonstrated by first obtaining the stability levels for the aircraft with installed lag dampers (adjusted to 6 percent critical in-plane damping) and high damping landing gear. Following stability checks of ground resonance characteristics and hover conditions, the high damping landing gear was replaced by the design gear, which has no damping for ground resonance purposes. The flight envelope for the YUH-61A was then expanded, demonstrating stability for climbs, descents, turns, forward speed, and various other conditions. From this work the critical flight conditions were determined. Finally, the damping of the lag damper was reduced by decrements of 2 percent critical damping until it was finally removed. The aircraft has now been flown to speeds beyond maximum level flight speed, V_H, at various gross weights, and under various maneuver conditions, and its stability has been demonatrated throughout.

YUH-61A Flight Test Stability Results

Ground resonance stability. Collective pitch sweeps were performed to investigate the ground resonance characteristics. These sweeps were made at three different rotor speeds, 94 percent N_R, 97 percent N_R, and 102 percent N_R. The test results performed at 97 percent N_R are shown in Figure 18. For this work, the aircraft was configured to design gross weight, with the design landing gear and the lag dampers removed. At all three speeds there is a trend of increasing stability as the collective is increased from 0 percent to 100 percent airborne. This increase equals 5.0 to 7.5 percent modal damping at each of the rotor speeds. In general, this is in good agreement with the earlier C-56 analysis results (Figure 7).

Air resonance stability. The investigation of air resonance as a function of airspeed was conducted as part of the envelope expansion program of the YUH-61A. The measured $\Omega-\omega_\zeta$ mode modal damping values for the YUH-61A is shown in Figure 19. As with the ground resonance work, the aircraft is configured to design gross weight with the lag dampers removed. As shown in this figure, the test values of the stability of the aircraft varies from about 7 percent modal damping in hover, out-of-ground effect, to a peak damping value of 12 percent critical near 80 percent V_H. In general, the damping is about level with airspeed. The minimum value at 106.5 percent V_H with the lag dampers removed is 7 percent. Notice that the trend in damping with airspeed matches data taken during the test of the 1.67 meter diameter Froude-scaled model (Figure 13), except that the magnitude of the test data is different because of lower inherent structural damping in the model.

CONCLUSIONS

Several conclusions can be drawn from this systematic approach to the aeroelastic stability problem of a soft in-plane hingeless rotor helicopter.

1. The YUH-61A has a stable soft in-plane hingeless rotor system.

2. The stable characteristics of the YUH-61A helicopter are attributed to the proper choice of the blade frequencies relative to the normal operating rotor speed and the hub parameters incorporated into the final design, such as zero precone of the blade feathering axis, and equivalent hinge sequence of pitch-flap-lag from inboard to outboard.

3. The sensitivities of stability to these parameters were analyzed by a 20 degree-of-freedom analysis and verified by two model tests.

4. A shake and decay technique was developed during a second, 1.67 meter diameter model test. This enabled the measurement of modal damping ratios, or the degree of stability, at every test point.

5. The test technique developed and perfected during model testing is useful for the in-flight shake test of the full scale helicopter. This technique, combined with the Grumman Automated Telemetry System, provides an efficient way to conduct the flight test program.

6. The in-flight shake test is the final step in the systematic approach to develop a rotor system free of aeroelastic instability when coupled to the airframe.

7. With an analytical tool substantiated by model testing, and the analytical trend study also verified by test, confidence can be placed in the predicted stability characteristics of a new vehicle. A flight program can be laid out, then, with minimum risk.

REFERENCE

1. Coleman, R.P.: Theory of Self-Excited Mechanical Oscillations of Hinged Rotor Blades. NACA ARR-3G29, July 1943.

2. Burkam, J.E.; and Miao, W.: Exploration of Aeroelastic Stability Boundaries with a Soft-in-Plane Hingeless-Rotor Model. Preprint 610, 28th Annual National Forum of the American Helicopter Society, May 1972.

3. Hohenemser, K.H.: Hingeless Rotorcraft Flight Dynamics, AGARD Publication, AGARD-AG-197, September 1974, pp. 25-27.

4. Lytwyn, R.T.; and Miao, W.: Airborne and Ground Resonance of Hingeless Rotors. Preprint 414, 26th Annual National Forum of the American Helicopter Society, June 1970.

5. Miao, Wen-Liu; and Huber, Helmut B.: Rotor Aeroelastic Stability Coupled With Helicopter Body Motion. NASA SP-352, 1974, pp. 137-146.

6. Marshall, D.L.; and Steinmann, H.H.: UTTAS Flight Test: Real-Time Data Analysis. 30th Annual National Forum of the American Helicopter Society, May 1974.

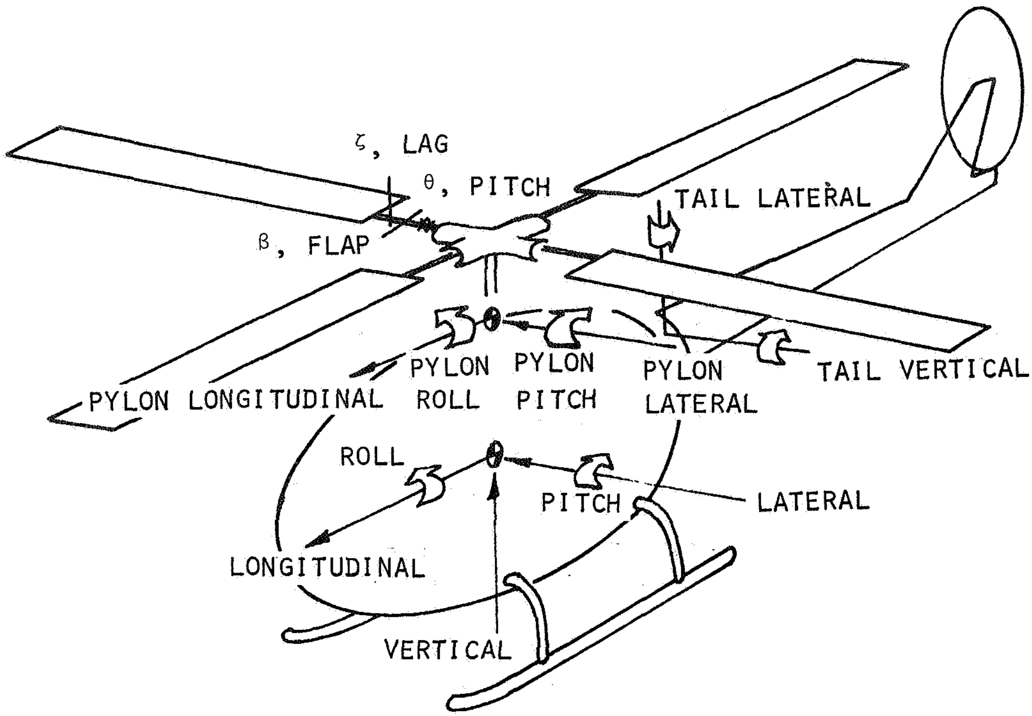

Figure 1. Coupled Rotor-Fuselage Analytical Model C-56.

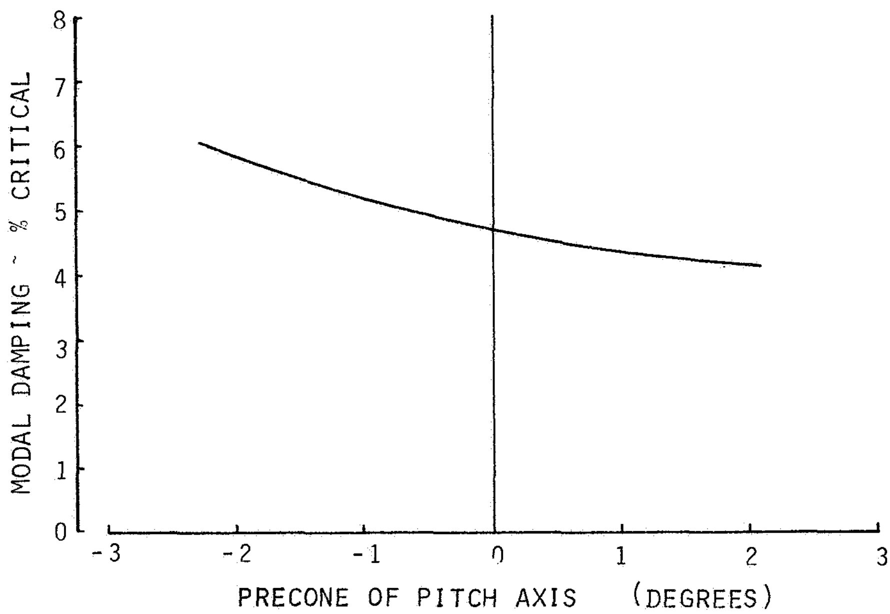

Figure 2. Effect of Precone on Air Resonance Stability.

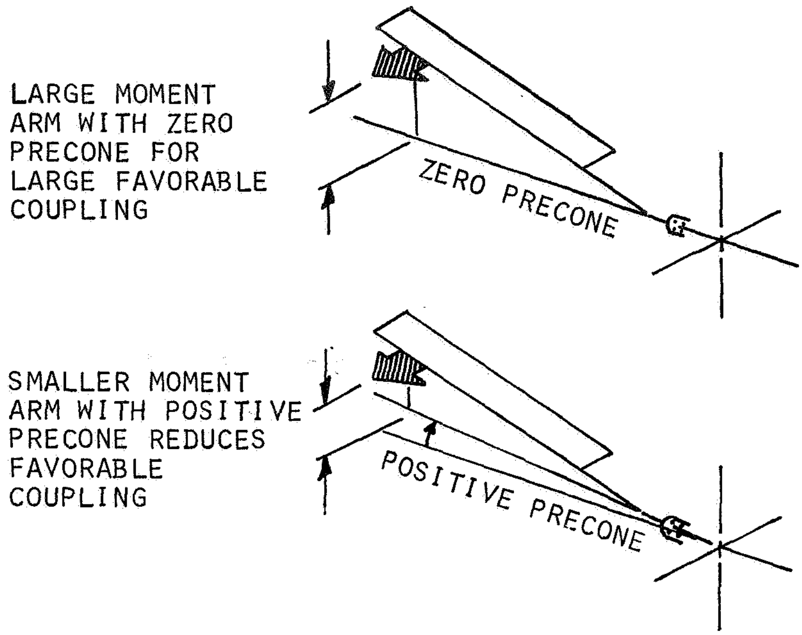

Figure 3. Effect of Precone in Reducing Favorable Flap-Pitch Coupling.

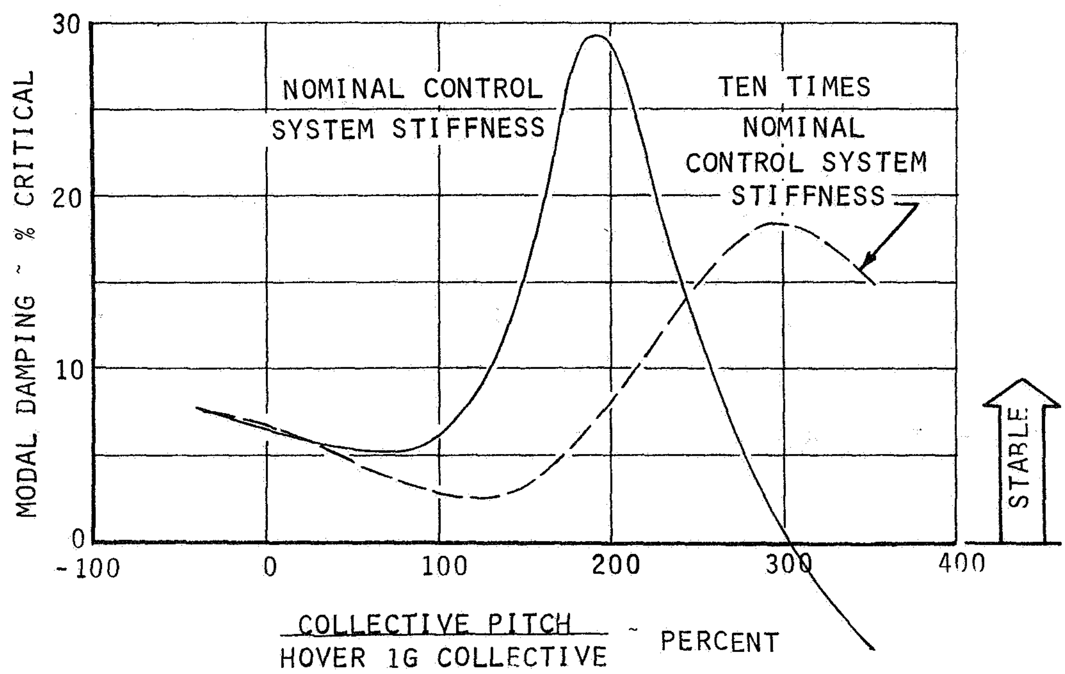

Figure 4. Effect of Control System Flexibility.

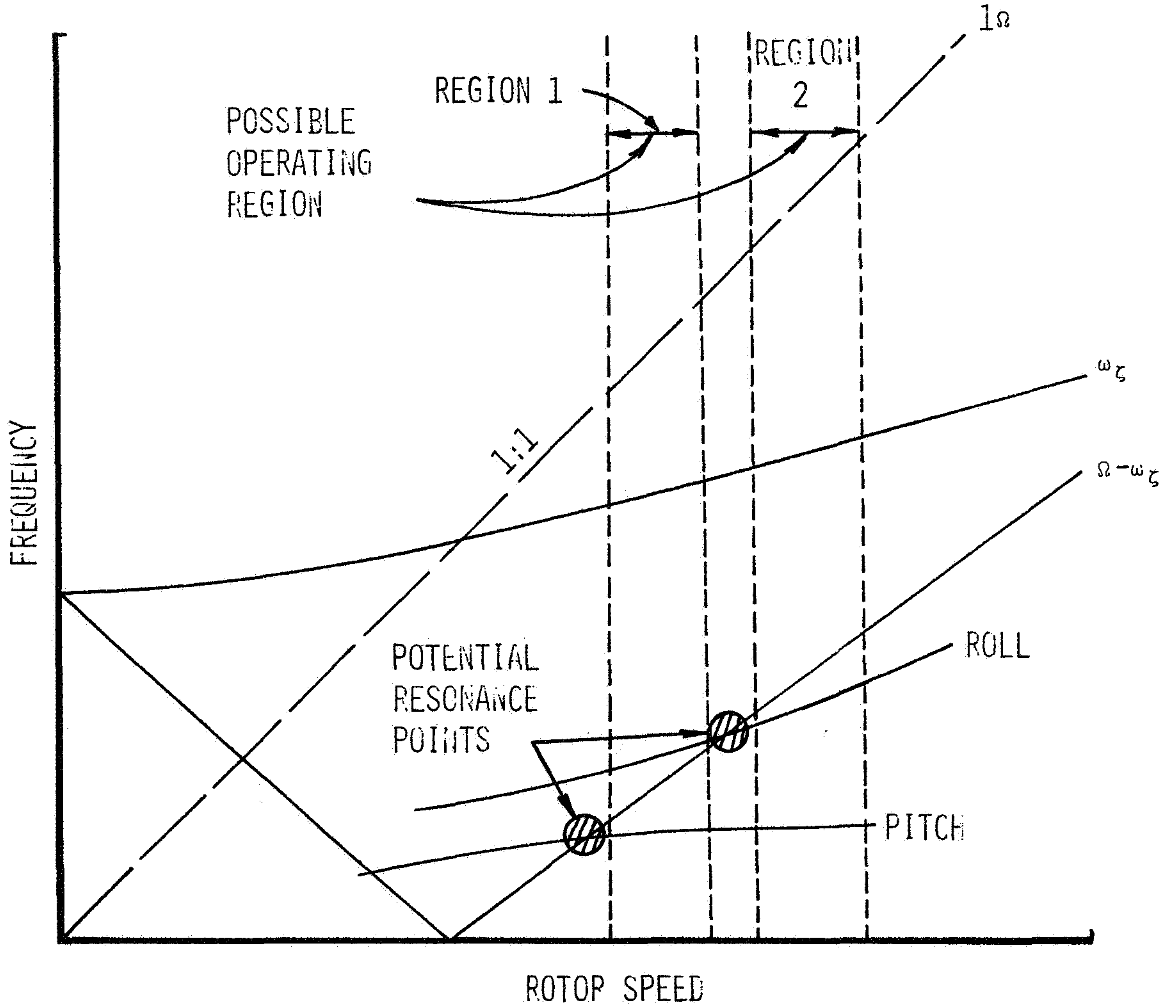

Figure 5. Potential Air Resonance Points and Operating Regions.

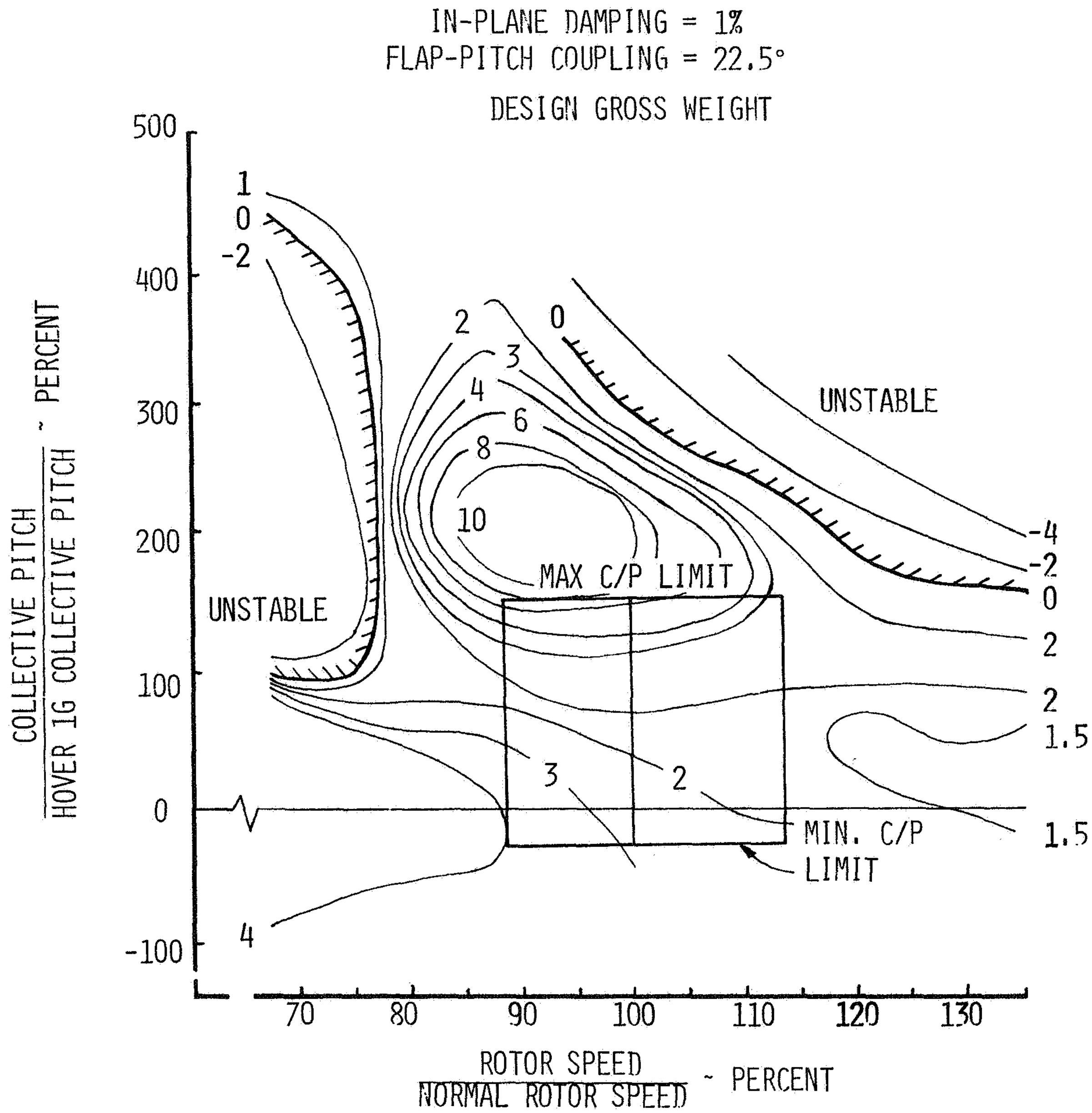

Figure 6. YUH-61A Air Resonance Characteristics.

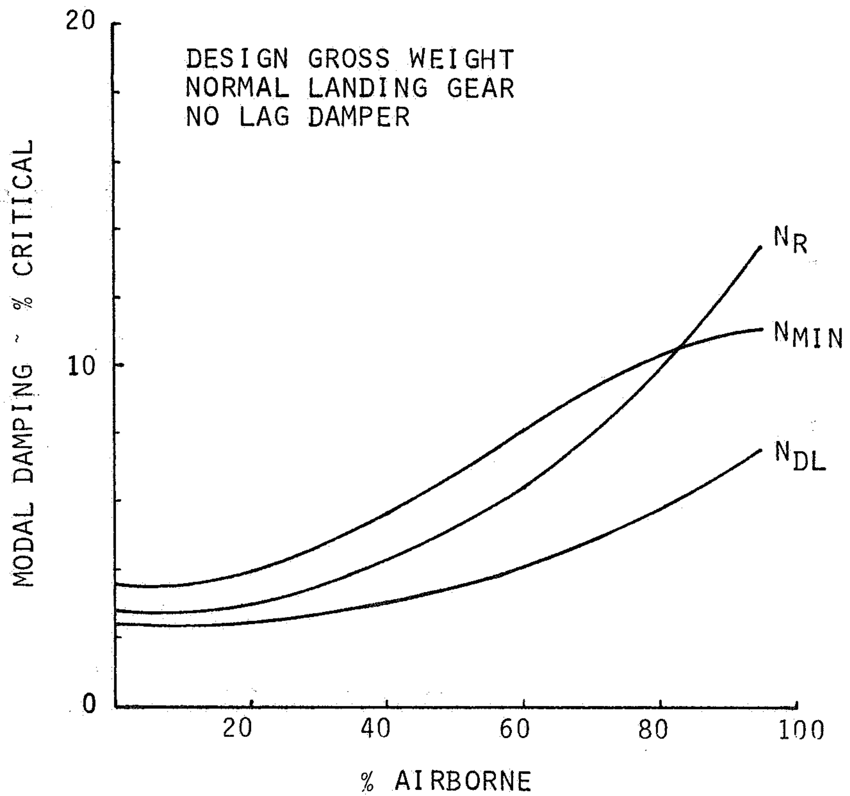

Figure 7. YUH-61A Ground Resonance Characteristics.

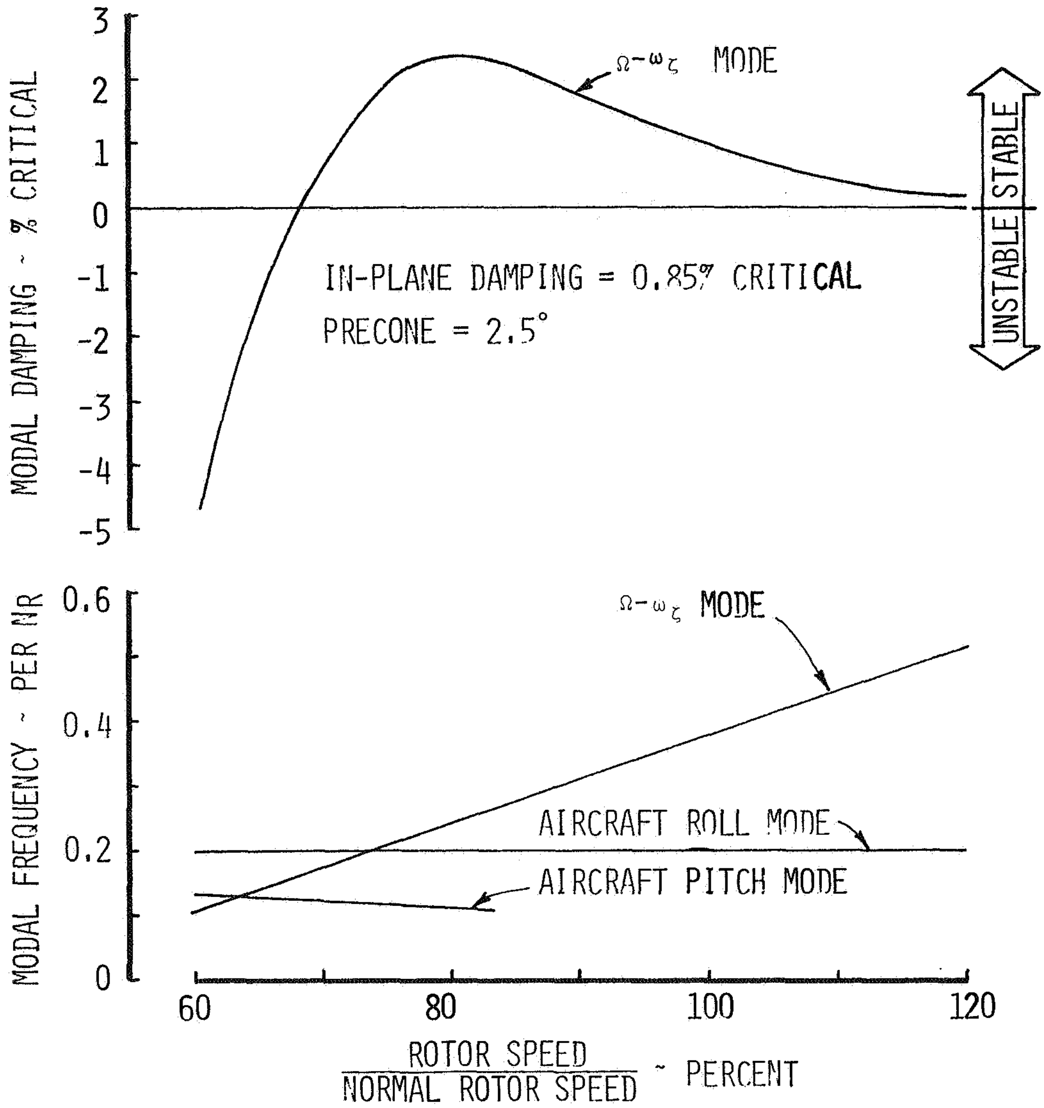

Figure 8. 1/13.8 Scaled BO-105 Model-Modal Frequencies and Damping.

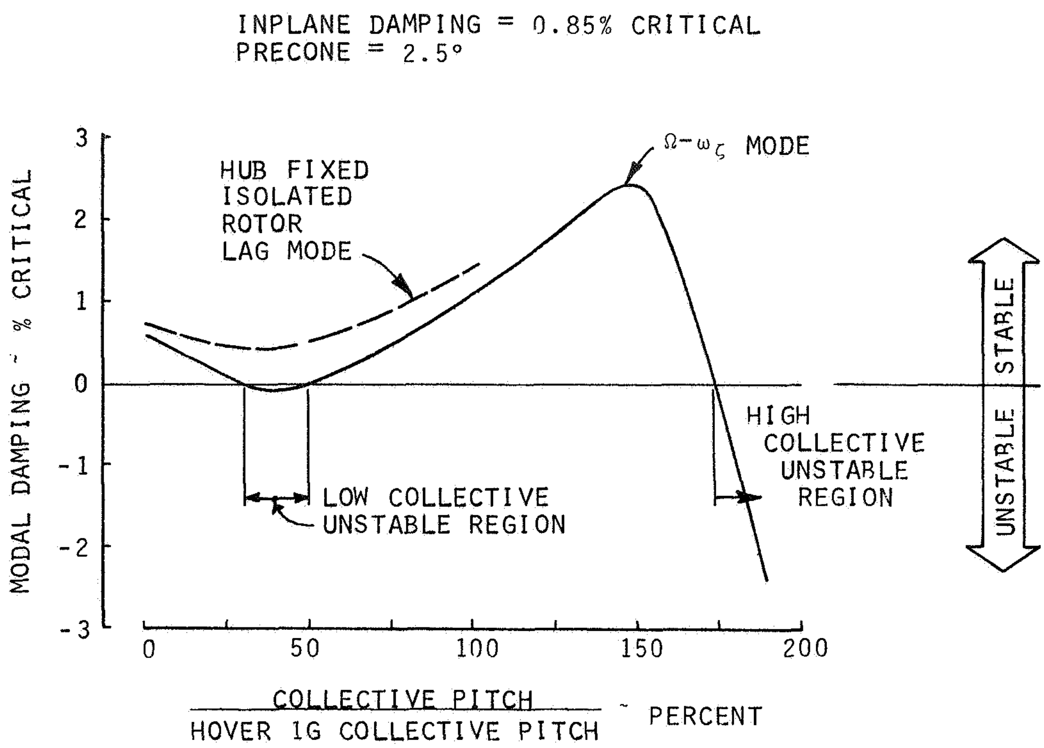

Figure 9. Thrust Effect on Stability.

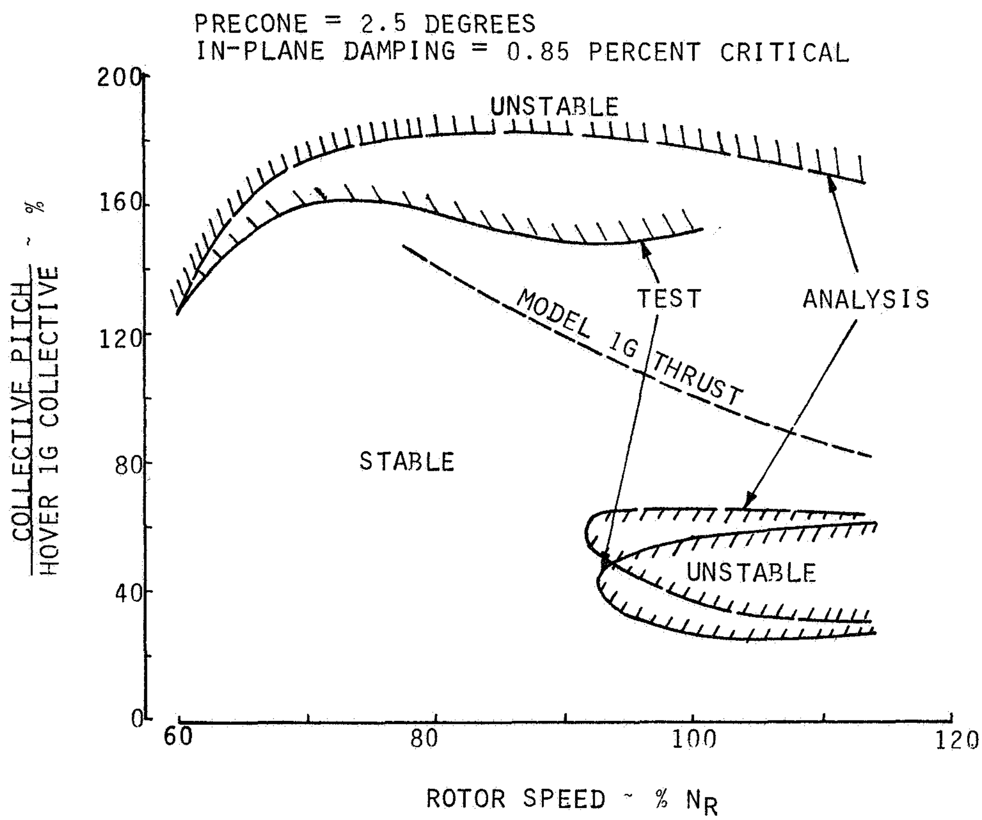

Figure 10. Stability Map of 1/13.8 Scaled BO-105 Model.

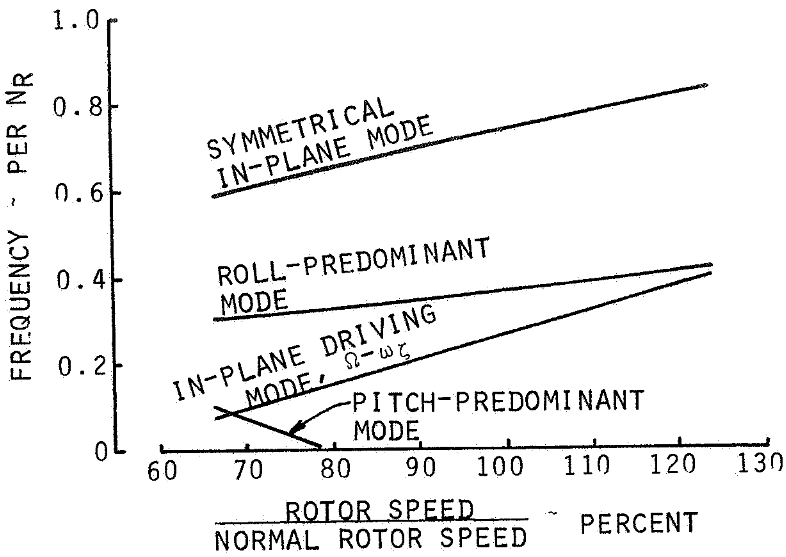

Figure 11. 1.67 Meter Diameter YUH-61A Model-Modal Frequencies.

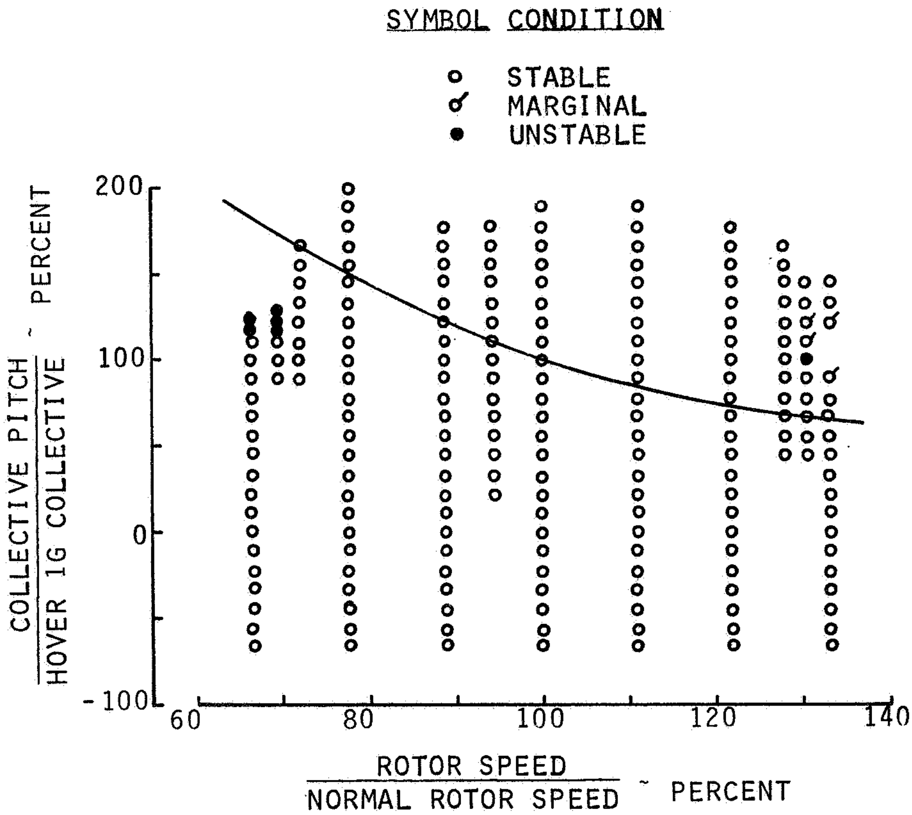

Figure 12. Map of Stability Test Points.

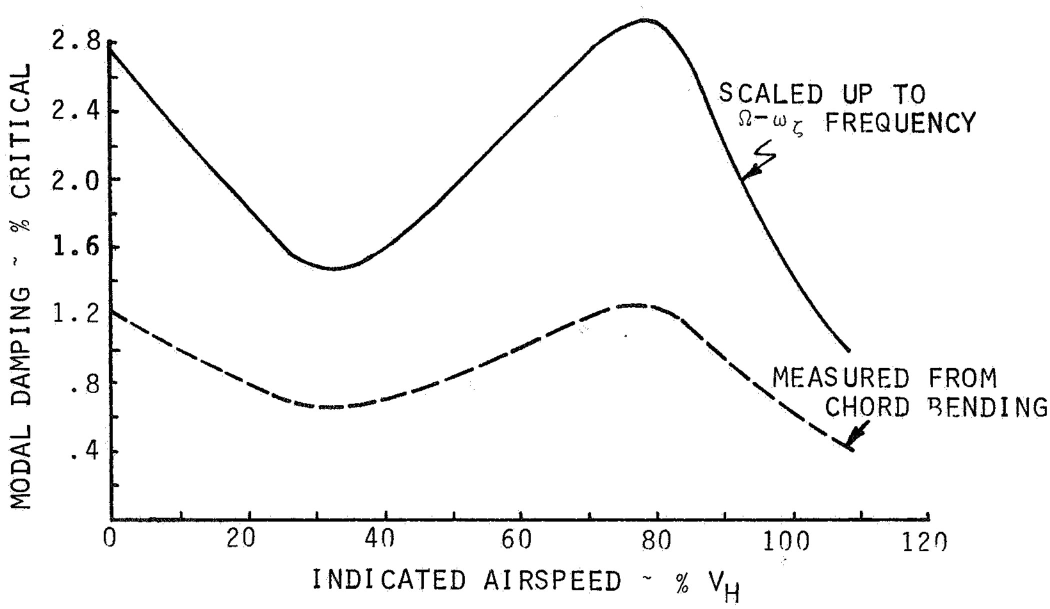

Figure 13. Stability in Forward Flight.

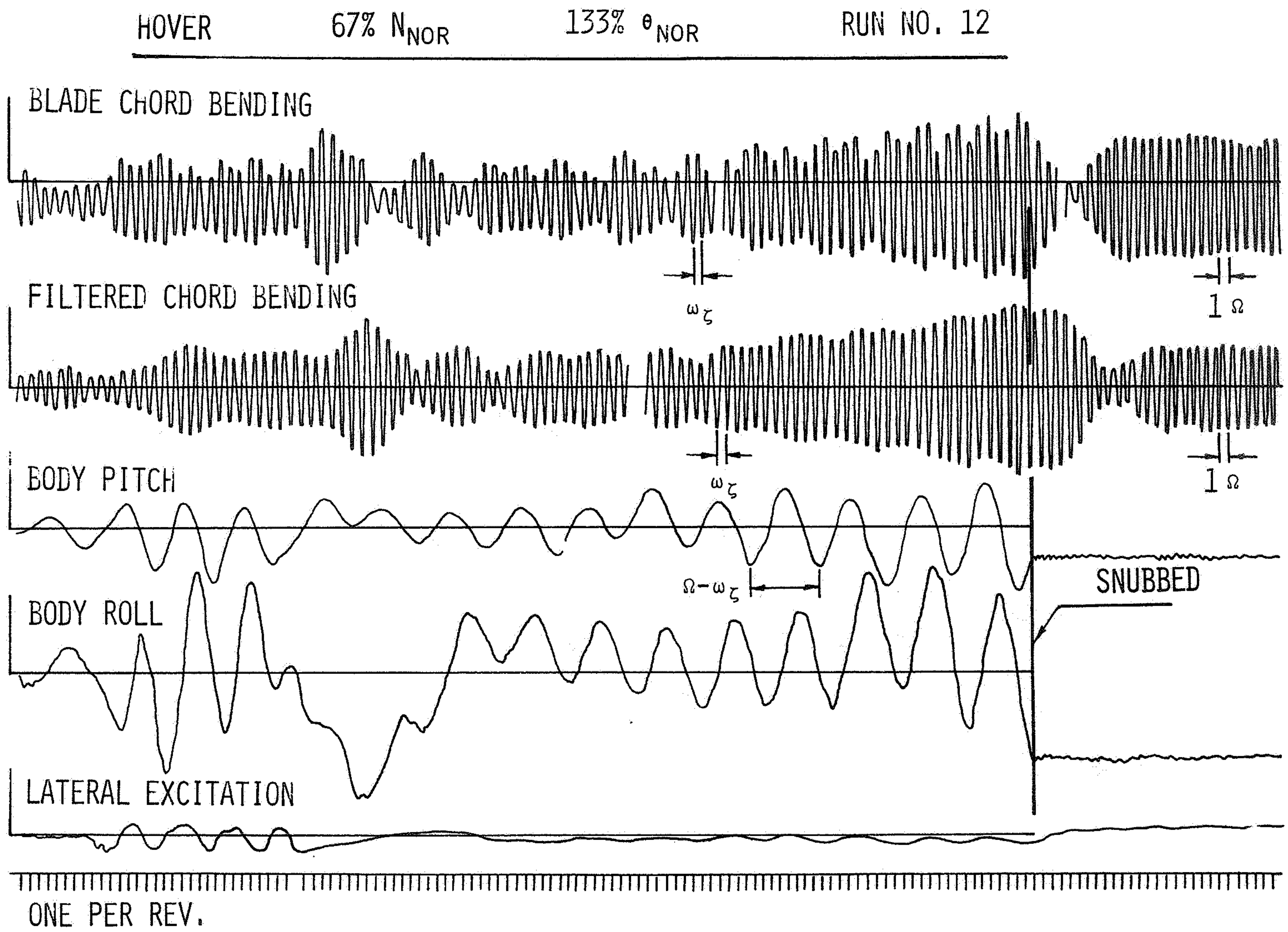

Figure 14. Typical Time History of 1.67 Meter Model.

Figure 15. YUH-61A Helicopter.

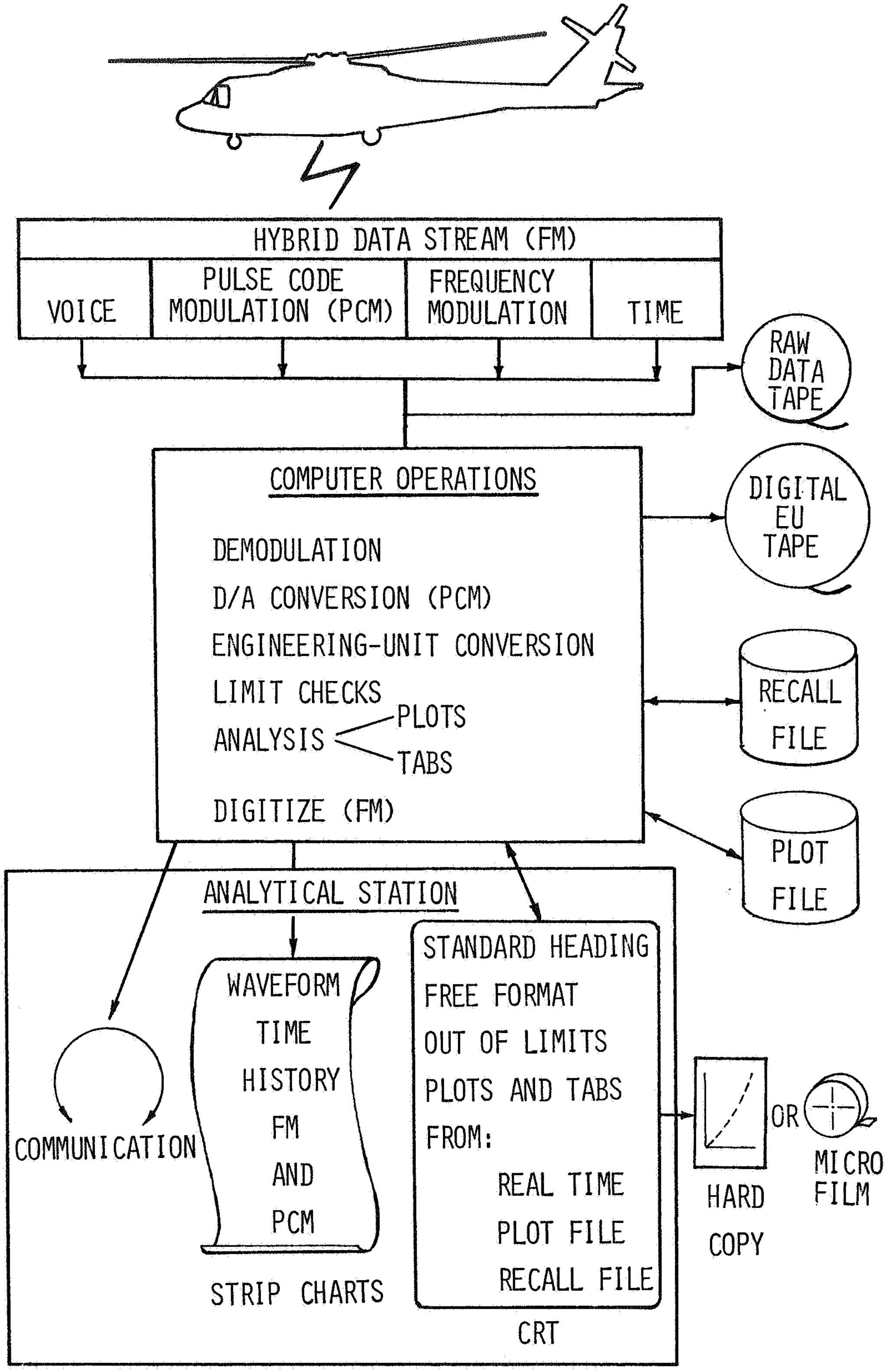

Figure 16. Schematic of Real-Time Data System.

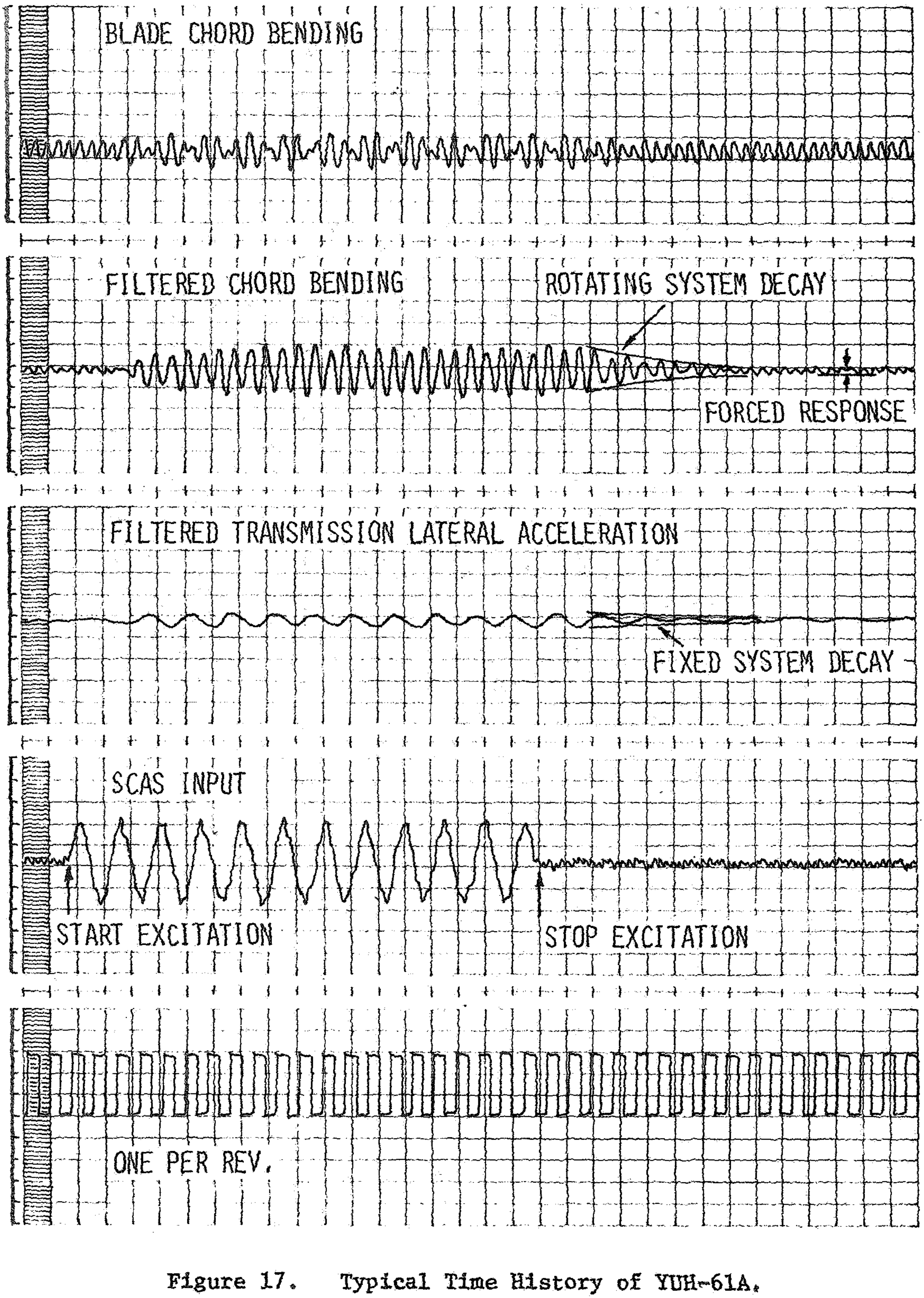

Figure 17. Typical Time History of YUH-61A.

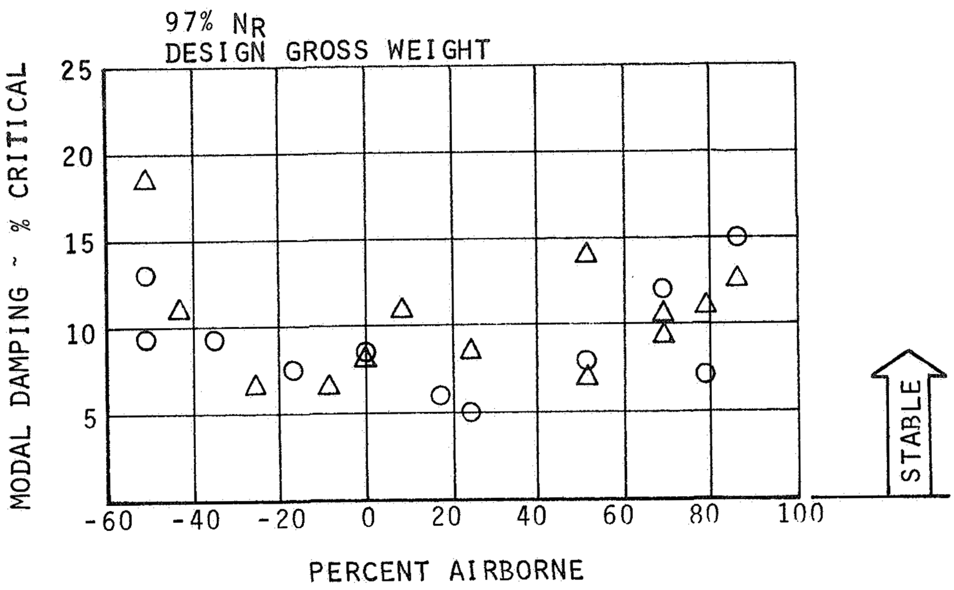

Figure 18. YUH-61A Ground Resonance Test Data.

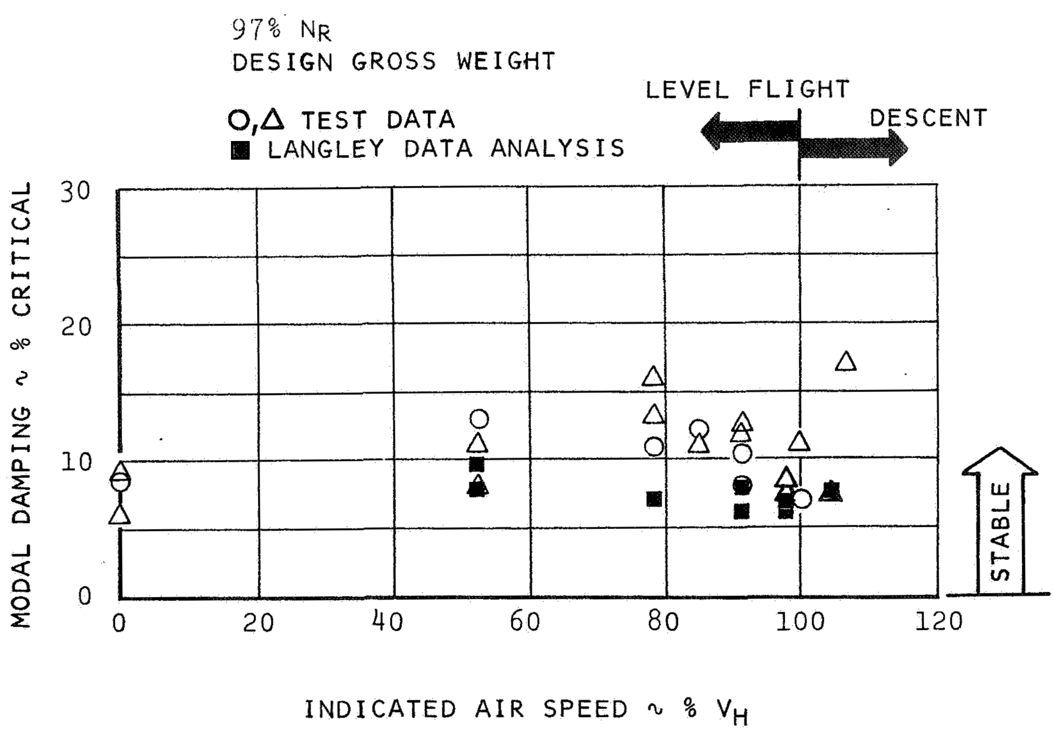

Figure 19. YUH-61A Air Resonance Test Data.